Catalysis Today 139 (2008) 196–201

Contents lists available at ScienceDirect

Catalysis Today

journal homepage: www.elsevier.com/locate/cattod

Nb-containing mesoporous materials of MCF type—Acidic and oxidative properties

Maciej Trejda [a,*], Jolanta Kujawa [a], Maria Ziolek [a], Julita Mrowiec-Białoń [b]

[a] Adam Mickiewicz University, Faculty of Chemistry, Grunwaldzka 6, PL-60-780 Poznan, Poland
[b] Institute of Chemical Engineering, Polish Academy of Science, Baltycka 5, 44-100 Gliwice, Poland

ARTICLE INFO

Article history:
Available online 20 May 2008

Keywords:
NbMCF
Pyridine adsorption
Methanol oxidation
Cyclohexene epoxidation

ABSTRACT

The new niobium-containing mesoporous catalysts based on MCF structure were prepared by niobium introduction *via* grafting and co-precipitation. The materials were characterised by N_2 adsorption, XRD, UV–vis, pyridine adsorption followed by FTIR and test reactions. Three various Nb precursors were applied: ammonium oxalate complex, ethoxide and chloride. It is documented by UV–vis that the best isolation of Nb species is reached when $NbO(C_2O_4)_2(NH_4)\cdot H_2O$ is applied for grafting and the same sample reveals the highest acidity determined by the test reaction—2-propanol conversion and pyridine adsorption combined with FTIR study. Niobium-containing MCF materials reveal both acidic and oxidative properties. The redox centres are active in the presence of oxygen and lead to very high selectivity in formaldehyde production from methanol. For liquid phase oxidation of cyclohexene with hydrogen peroxide both kinds of centres are active. Oxidative one causes the formation of epoxide, and acidic sites lead to the ring opening and diol production.

1. Introduction

Siliceous mesostructured cellular foams (MCF) are a relatively new class of porous materials with well-defined uniform ultralarge mesopores [1,2]. Their structure is templated by oil in water microemulsions. The catalytic activity of these materials were examined in different processes, e.g. esterification [3], selective oxidation of α-pinene [4]. Due to the presence of a well-defined large mesopore system this kind of materials can be attractive for processes in which the diffusion within the pores plays an important role, e.g. for the oxidation carried out in the liquid phase [5,6]. Since the discovery of mesoporous silicates in 1992 [7], designated as MCM-41, many works have been devoted to the synthesis of metallosilicates (TMCM-41) containing various transition metals and their application in liquid phase oxidations.

Mesoporous molecular sieves of M41S family (MCM-41 and MCM-48) have been modified by transition metals *via* post synthesis grafting or tethering, or *via* inclusion of metal during the synthesis (co-precipitation). The nature of metal active species depends on metal location (extra-framework or framework positions). Location of metal and sizes of metal clusters can affect the diffusion effect (e.g. the accessibility of reactant molecules to metal active sites) [5,6].

There is no doubt that TS-1 is still the best heterogeneous catalyst for many oxidation processes carried out in the liquid phase. However, due to the diffusion limitation there is still a need to look for the materials containing larger pores. Therefore, the focus of many researchers was on the preparation of Ti-containing mesoporous materials [8–13]. However, the disadvantage in using such materials in the liquid phase oxidation is their low hydrophobicity, which is important when diluted hydrogen peroxide is used as an oxidant. Corma et al. [14] proposed two strategies to improve the catalytic activity of TiMCM-41 in the epoxidation of olefins. The first involves the increase of the hydrophobicity of the material *via* silylation of the catalyst surface, and the second is based on the removal of water from the reaction media.

Instead of TiMCM-41 modification *via* silylation necessary for the improvement of epoxidation activity one can look for mesoporous materials containing other active metal species, giving rise to a different reaction pathway or to increase of hydrophobicity. NbMCM-41 and NbSBA-15 seem to be very useful catalysts for epoxidation of olefins [15–18]. The increase of Nb content caused the enhancement of selectivity to epoxide on NbMCM-41 samples [16]. However, in the case of NbMCM-41 mesoporous molecular sieves the growth of niobium content led

* Corresponding author. Tel.: +48 61 8291243; fax: +48 61 8658008.
E-mail address: tmaciej@amu.edu.pl (M. Trejda).

0920-5861/$ – see front matter © 2008 Elsevier B.V. All rights reserved.
doi:10.1016/j.cattod.2008.04.006

also to the increase of Nb species in the extra-framework location. This kind of species can be easier leached into the solution and can increase undesired selectivity to diols. Therefore, still there is room for looking for the other mesoporous catalysts.

The idea of this work was to prepare mesoporous materials which posses different structural properties compared to samples examined before. The MCFs materials composed of uniformly sized, large spherical cells that are interconnected by uniform windows to create a continuous 3D pore system [1]. This interconnected nature can be very attractive and makes the MCFs materials promising candidates for supports of catalysts. This structure differs from parallel mesopores in MCM-41 and SBA-15 type materials. Moreover, the new structure of host material can generate a different surrounding for niobium species and therefore create new properties of active species. In this work three different sources of niobium were used for the modification of MCF siliceous foams. Metal precursors were introduced into the solid *via* grafting method. Additionally, for the stabilization of active species in liquid phase reactions, the catalysts were also prepared *via* co-precipitation technique. We have expected that this method will enhance the isolation of niobium species, which is an important factor in the cyclohexene epoxidation process [5]. The characterisation of prepared materials and their catalytic activity in gas and liquid phase reactions are presented and discussed in this paper.

2. Experimental

2.1. Catalyst preparation

For the preparation of siliceous MCFs a typical procedure have been used [2]. Surfactant, Pluronic P123 (0.4 mmol), was dissolved in 1.6 M HCl (75 cm^3) at room temperature. 1,3,5-Trimethylbenzene (17 mmol) and NH_4F (0.6 mmol) were added under vigorous stirring. Then the mixture was heated to 333 K. Following 1 h of stirring TEOS was added (4.4 g) to obtain solution A. Then A was stirred for 2 h and stored at 333 K for 20 h and subsequently at 373 K for 24 h. After cooling to room temperature, the precipitate was isolated by filtration, dried at room temperature for 4 days and calcined in air at 773 K for 8 h.

Nb-MCFs were prepared by the direct incorporation of the niobium precursor during the synthesis of MCFs (co-precipitation method) or by the post synthesis procedure to obtain samples with Si/Nb molar ratio of about 30. In both methods three niobium precursors were used: $NbO(C_2O_4)_2(NH_4)\cdot H_2O$ (I), $NbCl_5$ (II) and $Nb(OC_2H_5)_5$ (III). All compounds were from Aldrich.

In the co-precipitation procedure a suitable amount of the niobium precursor, dissolved in 5 cm^3 of solvent, was added dropwise to solution A after addition of TEOS and then the procedure was the same as for the siliceous MCFs. To obtain NbMCF-1 sample 0.307 g of (I) was dissolved in 5 cm^3 of methanol. In the case of NbMCF-2 and NbMCF-3, 0.187 g of (II) and 0.175 cm^3 of (III), respectively, were dissolved in 5 cm^3 of ethanol.

Before grafting of niobium, pristine MCFs were contacted overnight with water vapour at room temperature followed by calcination at 473 K for 2 h. The silanols concentration, determined by the thermogravimetric method [19], was ca. 3 OH/nm^2. Niobium precursor was dissolved in 30 cm^3 of solvent, 1 g of siliceous MCF was dispersed therein and the mixture was reflux for 24 h prior to the removal of solvent by evaporation at 323 K. Finally the samples were calcined at 773 K for 8 h under air flow. Three samples NbMCF-4, NbMCF-5 and NbMCF-6 were obtained using 0.247 g of (I) dissolved in methanol, 0.15 g of (II) dissolved in ethanol and 0.14 cm^3 of (III) dissolved in hexane.

2.2. Catalyst characterisation

N_2 adsorption/desorption isotherms were obtained in a Micromeritics ASAP equipment, model 2010. The samples (200 mg) were pre-treated *in situ* under vacuum at 573 K for 3 h. The surface area was calculated using the BET method. The pore size distributions (PSDs), the pore sizes (the maximum of the PSD), and the mesopore volumes were determined from the adsorption branch of isotherms.

UV–vis spectra were registered using a Varian-Cary 300 Scan UV–vis spectrophotometer. Catalyst powders were placed into the cell equipped with a quartz window. The Kubelka–Munk function ($F(R)$) was used to convert reflectance measurements into equivalent absorption spectra using the reflectance of SPECTRALON as a reference.

The surface properties were characterised by pyridine adsorption followed by FTIR spectroscopy and by 2-propanol conversion.

Infrared spectra were recorded with a Bruker Vector 22 FTIR spectrometer using an *in situ* cell. Samples were pressed under low pressure into a thin wafer of ca. 6 mg cm^{-2} and placed inside the cell. Catalysts were evacuated at 673 K during 2 h and pyridine (PY) was then admitted at 373 K. After saturation with PY the samples were degassed at 373, 423, 473, and 523 K in vacuum for 30 min. Spectra were recorded at room temperature in the range from 4000 to 400 cm^{-1}. The spectrum without any sample (''background spectrum'') was subtracted from all recorded spectra. The IR spectra of the activated samples (after evacuation at 673 K) were subtracted from those recorded after the adsorption of PY followed by various treatments. The reported spectra are the results of this subtraction.

The 2-propanol conversion (dehydration and dehydrogenation) was performed, using a microcatalytic pulse reactor inserted between the sample inlet and the column of a CHROM-5 chromatograph. The catalyst bed (0.02 g with a size fraction of $0.5 < Ø < 1$ mm) was first activated at 673 K for 2 h under helium flow (40 cm^3 min^{-1}). The 2-propanol (Aldrich) conversion was studied at 423, 473 and 523 K using 3 μl pulses of alcohol under helium flow (40 cm^3 min^{-1}). The reactant and reaction products: propene, 2-propanone (acetone) and diisopropyl ether were analysed using CHROM-5 gas chromatograph on line with microreactor. The reaction mixture was separated on 2 m column filled with Carbowax 400 (80–100 mesh) at 338 K in helium flow (40 cm^3 min^{-1}) and detected by TCD.

2.3. Methanol oxidation

Reactions were performed in a fixed-bed flow reactor. The pressed materials were granulated to $0.5 < Ø < 1$ mm size fraction. 0.02 g of the catalysts (calculated for the dehydrated materials) were placed into the reactor. The samples were activated in helium flow (40 cm^3 min^{-1}) at 723 K for 2 h. Next the temperature was decreased to 573 K. The gas mixture of CH_3OH and O_2, diluted by He, was used for the oxidation process with a total flow rate of 40 cm^3 min^{-1}. The reactor effluent was analysed using an online gas chromatograph (SRI 8610 GAS) with FID and TCD detectors. Hydrogen was used as a carrier gas. Substrates and products were separated on a 30 m column filled with GS-Q. The column was heated as follows: at 308 K for 40 min, then 10 K min^{-1} up to 508 K. Following products were analysed: formaldehyde, dimethyl ether, methyl formate and methylal.

2.4. Oxidation of cyclohexene with hydrogen peroxide

The reaction was performed at 313 K in the liquid phase using acetonitrile as a solvent. The catalytic reaction between cyclohex-

Table 1
Preparation and texture parameters of the samples

Catalyst	Niobium incorporation technique	Nb precursor	BET area ($m^2\ g^{-1}$)	Pore volume[a] ($cm^3\ g^{-1}$)
MCF-1[*]			560	1.90
MCF-2[**]			600	2.40
NbMCF-1	Grafting	$NbO(C_2O_4)_2(NH_4)\cdot H_2O$	430	1.56
NbMCF-2	Grafting	$NbCl_5$	460	1.72
NbMCF-3	Grafting	$Nb(OC_2H_5)_5$	450	2.08
NbMCF-4	Co-precipitation	$NbO(C_2O_4)_2(NH_4)\cdot H_2O$	700	2.35
NbMCF-5	Co-precipitation	$NbCl_5$	730	1.70
NbMCF-6	Co-precipitation	$Nb(OC_2H_5)_5$	710	1.63

[a] BJH desorption pore volume.
[*] The support for NbMCF-1 and NbMCF-2.
[**] The support for NbMCF-3.

ene and hydrogen peroxide was carried out in a glass flask equipped with a magnetic stirrer, a thermocouple, a reflux condenser and a membrane for sampling. 0.04 g of a calcined catalyst was placed into the flask and the solvent was added. The oxidation was conducted by efficient stirring of a mixture of a solvent and a catalyst at 313 K. After stirring for 15 min at 313 K, cyclohexene (2 mmol) was added, followed by the dropwise addition of ~35% hydrogen peroxide (2 mmol). Samples were withdrawn at regular time intervals and analysed by a gas chromatograph GC 8000 Top equipped with a capillary column DB-1 attached to a FID, operated with a heating program: 340 K for 15 min, ramp 10 K min^{-1} to 360 K (kept for 13 min). Following products were analysed: epoxide, 1,2-dicyclohexanol, cyclohexanol, cyclohexanone, cyclohexenol, cyclohexenone.

3. Results and discussion

3.1. Texture/structure characterisation

The list of catalysts prepared within this work as well as their textural characterisation are shown in Table 1. Based on the niobium incorporation technique the samples can be divided into two groups. First group contains materials with niobium introduced after the synthesis of mesoporous foams, i.e. *via* grafting. In the second group the niobium precursors were added into the synthesis mixture, i.e. they were included *via* co-precipitation. Different sources of niobium were applied (niobium ammonium oxalate, niobium chloride and niobium ethoxide) for both preparation methods. All the materials are mesoporous, as one can deduce from N_2 adsorption/desorption isotherms (Fig. 1). The isotherms are of type IV according to the IUPAC classification. All of them exhibit the H1-type hysteresis loop, which is typical of large-pore mesoporous solids. The hysteresis loop is much narrow in the case of materials prepared *via* grafting (Fig. 1a–c) showing the more uniform pore size distribution. It can be caused by the well-ordered siliceous support for Nb species. These two groups of materials do not show the same textural properties. The samples prepared *via* grafting of niobium species posses the much lower surface areas. This difference can be explained by filling the pores with niobium compounds and finally location of bulk Nb species on the wall, that decreases the surface area. Moreover, it can be also caused by a partial breakdown of the porous silica structure during the grafting or calcination process. Nevertheless, it is worthy to point out that the surface areas of siliceous mesoporous foams (before grafting) are in the range of 560–600 $m^2\ g^{-1}$. It can be suggested that the preparation of niobium-containing MCFs *via* co-precipitation significantly enhances the surface areas. It could happen for example when the niobium species are incorporated in the material walls.

The state of niobium species on catalyst surface is crucial for the catalytic activity. For estimation of kinds of niobium species the UV/vis technique has been applied. The spectra of samples prepared *via* grafting are shown in Fig. 2. The first very important finding is the lack of a band at ca. 330 nm, which is a characteristic for octahedral niobium oxide species in the extra-framework position [20]. The same information was given from XRD patterns on which any crystal phases were observed in the high-angle range (not shown here). The main band in Fig. 2 seems to consist of two different bands with maximum ca. 228 and 250 nm, as it is shown for the NbMCF-2 (Fig. 2, deconvolution). These two species seems to be tetrahedrally coordinated with various ligands. It is interesting that the NbMCF-1, prepared from niobium ammonium oxalate exhibits the domination of one band at 228 nm. It means that this precursor containing a bulky ligand prefers niobium location only in one specific site, which seems to be isolated. This

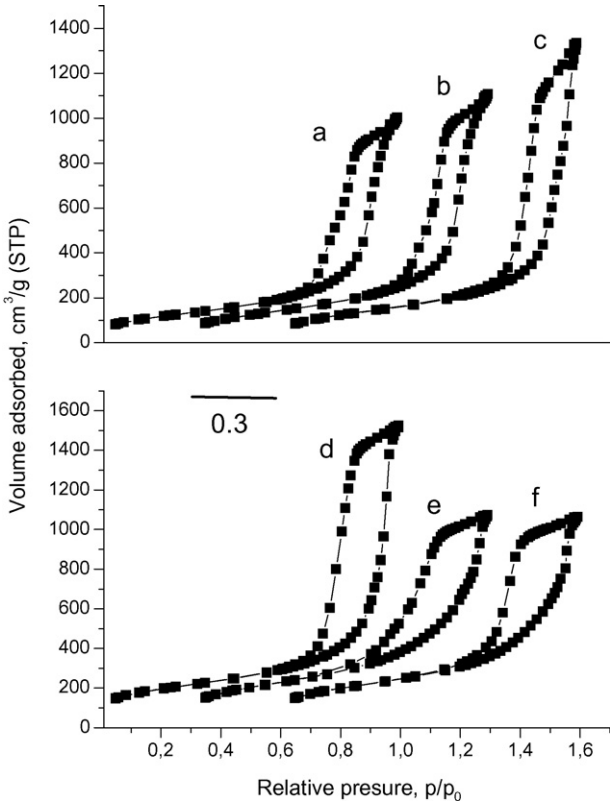

Fig. 1. N_2 adsorption/desorption isotherms of (a) NbMCF-1, (b) NbMCF-2, (c) NbMCF-3, (d) NbMCF-4, (e) NbMCF-5, and (f) NbMCF-6.

Table 2
Number of BAS and LAS calculated per 10 mg of the catalysts on the basis of IR bands observed after desorption of pyridine at 473 K and extinction coefficient of pyridine

Sample	Number of LAS[a] ($\times 10^{17}$)	Number of BAS[b] ($\times 10^{17}$)	Total number of acid sites ($\times 10^{17}$)
NbMCF-1	0.116	0.004	0.120
NbMCF-2	0.026	–	0.026
NbMCF-3	0.034	0.0006	0.035

[a] Extinction coefficient, $\varepsilon_{1450} = 1.5\ \mu mol^{-1}$ cm.
[b] Extinction coefficient, $\varepsilon_{1550} = 1.8\ \mu mol^{-1}$ cm.

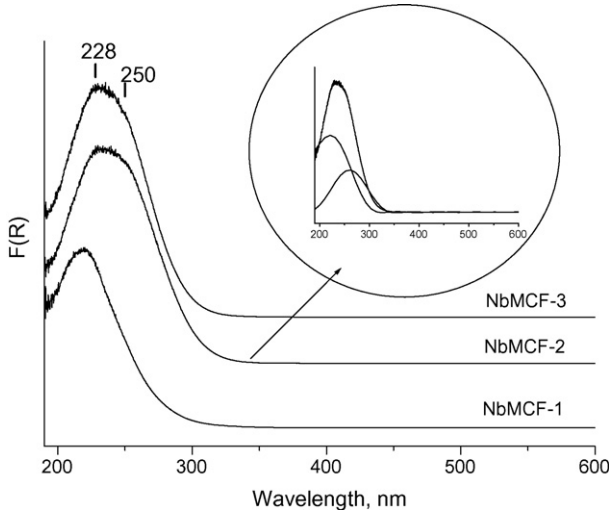

Fig. 2. UV/vis spectra of prepared samples (curve-fitting, Gauss fit).

phenomena will be also discussed during the presentation of acidity measurements.

3.2. Acidity measurements

For the evaluation of the amount and type of acidic centres, infrared spectroscopy combined with the adsorption of pyridine has been applied. The interaction of pyridine with Lewis acid sites (LASs) leads to appearing of the bands at ~1450 and 1610 cm^{-1} [21,22]. The intensity of the first one is related to the number of LAS whereas the position of the second band characterises the strength of LAS. Adsorption of pyridine on Brønsted acid sites (BAS) gives a band at 1550 cm^{-1} and two others in the 1620–1640 cm^{-1} range.

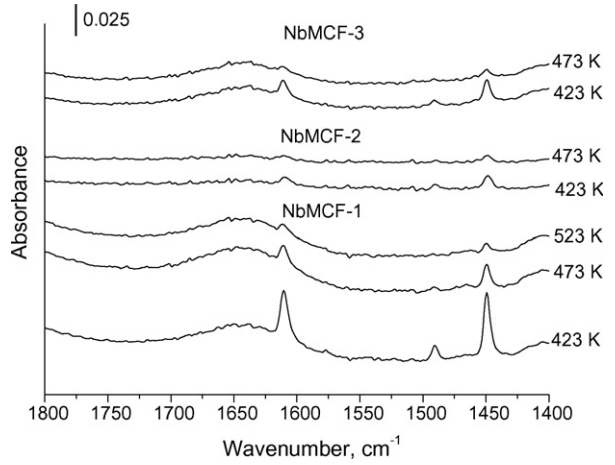

Fig. 3. FTIR spectra of pyridine desorption (calculated per 6 mg of the samples) at various temperatures (30 min at each temperature under vacuum).

The number of LAS and BAS as well as a total number of acid sites for the samples prepared *via* grafting are given in Table 2. In spite of the same amount of incorporated niobium species the materials possess a different number of acid sites and they can be ordered in the following sequence: NbMCF-1 > NbMCF-3 > NbMCF-2. In the same order one can locate the niobium precursors regarding the size of metal ligands: niobium ammonium oxalate (for NbMCF-1) > niobium ethoxide (for NbMCF-3) > niobium chloride (for NbMCF-2). The size of metal ligand seems to have an impact on the kind of niobium species present on material surface. The smaller ligand the shorter possible distance between metal atoms occurs. This enhances the agglomeration process which occurs on the material surface during the thermal treatment and finally decreases the number of niobium species accessible for the reactants. The better isolation which is postulated for NbMCF-1 sample has also an influence on the strength of the sites as it is shown in Fig. 3. Whereas for NbMCF-2 and NbMCF-3 samples the evacuation at 473 K leads to almost complete desorption of pyridine, the bands at 1610 and 1450 cm^{-1} are still present after evacuation at 523 K in the case of NbMCF-1 material.

The 2-propanol conversion can be used as a test reaction for the characterisation of acidic (Brønsted or Lewis) and/or basic properties of the solids [23,24]. Dehydration of alcohol to propene requires acidic centres, the formation of diisopropyl ether involves pairs of Lewis acid–base sites, whereas the dehydrogenation to acetone occurs on basic centres.

All catalysts prepared *via* grafting technique were examined in this process and their activity, i.e. conversion of alcohol at 473 K is presented in Fig. 4 together with the plot of the number of acid centres calculated from pyridine adsorption combined with FTIR study (Table 2). Propene was the only product observed during the reaction, so the conversion of isopropanol corresponds well to the yield of propene. This behaviour points out on the acidic character of all the materials, therefore one can expect the correlation between the conversion of isopropanol and number of acid sites.

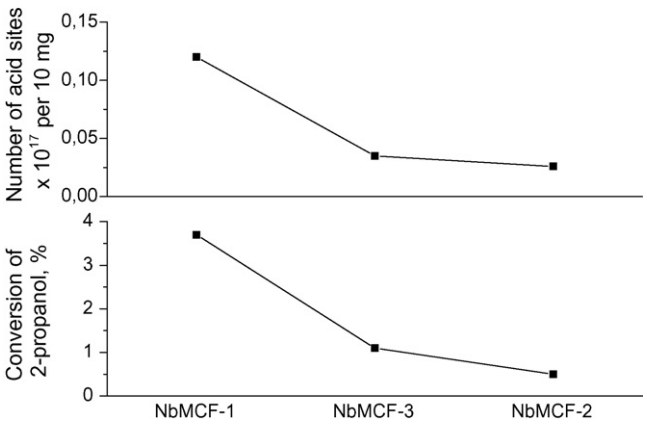

Fig. 4. Activity in 2-propanol decomposition (carried out at 473 K) and number of acid sites (from pyridine adsorption and evacuation at 473 K and FTIR study).

Table 3
The activity and selectivity in CH_3OH oxidation process carried out at 573 K

Catalyst	Conversion of CH_3OH (%)	Selectivity (%)		
		HCHO	$(CH_3)_2O$	$HCOOCH_3$
NbMCF-1	35	91	5	4
NbMCF-2	34	92	7	1
NbMCF-3	45	97	3	–

Indeed, the activity of catalysts in 2-propanol decomposition depends on the number of acid sites and increases with this number (Fig. 4). Interestingly both curves in Fig. 4 reveal the same slope.

3.3. Methanol oxidation

The use of methanol oxidation process is a good choice for the characterisation of both redox and acidic properties of the catalyst [25–27]. The redox centres are involved in the oxidation of alcohol towards formaldehyde. Dimethyl ether formation requires the acidic centres, whereas the other products are formed with the participation of both, redox and acidic centres. Therefore, the oxidation of methanol can give an information regarding the active sites on the catalyst surface.

The activity and selectivity of niobium-containing mesoporous foams in the methanol oxidation process carried out at 573 K are shown in Table 3. Two of the prepared samples (NbMCF-1 and NbMCF-2) showed similar activity, i.e. ca. 35% of conversion, whereas NbMCF-3 was a little more active. However, in the case of all the samples a high selectivity towards formaldehyde was observed. It is an important finding, because the formation of this product requires a presence of redox centres. Niobium species present on the material surface can serve both as a redox and as an acid sites. The domination of formaldehyde among the reaction products shows that in this reaction niobium species acts as redox sites. This can explain why the samples which differ in number of acid sites do not show the similar order of activity like in the case of isopropanol decomposition process. In fact the acidity of the samples does not play a crucial role in the methanol reaction with oxygen, because formaldehyde is the main product. Thus, in the presence of oxygen the redox character of the catalysts surface is evidenced.

3.4. Cyclohexene oxidation

The oxidation of cyclohexene has been applied to examine the properties of the prepared materials in liquid phase reactions. For this purpose an additional series of catalysts has been used, namely that prepared *via* co-precipitation. The co-precipitation technique for the preparation of metallosilicate mesoporous materials usually gives a better isolation of metal active species which is obviously crucial in the cyclohexene epoxidation process [5,6]. The acidic character of the materials can be deduced from the selectivity to diol [5]. However, one should remember that diols are easily formed in the homogeneous system (liquid) and therefore their formation can suggest also the leaching of active phase to the solution. The results of cyclohexene oxidation carried out at 313 K for 40 h are shown in Table 4.

Table 4
Conversion and selectivity in oxidation of cyclohexene carried out at 313 K after 40 h

Catalyst	Conversion and selectivity (%)					
	Cyclohexene	Epoxide	Diol	Cyclohexanol	Cyclohexenol	Other[a]
NbMCF-1	61	9	66	6	15	4
NbMCF-2	56	10	53	10	26	2
NbMCF-3	70	6	69	5	14	6
NbMCF-4	35	36	54	6	4	–
NbMCF-5	56	45	46	3	6	–
NbMCF-6	33	37	52	6	5	–

[a] Cyclohexenone and cyclohexanone.

The activity and the selectivity of prepared materials differ for both groups of catalysts. Whereas the samples prepared *via* grafting show a higher activity the niobium-containing mesoporous foams obtained *via* co-precipitation method manifest in much higher epoxidation selectivity. The presence of niobium dimmers or oligomers on the support is responsible for hydrogen peroxide decomposition and therefore creation of radical species. This radical species is not selective in the oxidation process and leads to the decrease of epoxide formation. It is important to stress that niobium dimmers (or oligomers) are present after grafting, whereas co-precipitation leads to the isolation of Nb species [5].

As it was mentioned above, the creation of epoxide requires the isolation of niobium species on the mesoporous catalyst surface [5]. Contrary to the activity, the selectivity to epoxide for second series of catalysts, prepared by adding the niobium precursor directly into the synthesis gel, was ca. 4–5 times higher than that registered for the grafted samples. When the selectivity for epoxide in the case of NbMCF-5 reached 45%, the most selective material prepared *via* niobium grafting showed 10% selectivity to epoxide (NbMCF-2). This phenomena clearly shows the better isolation of niobium centres located in the skeleton if Nb source is added to the synthesis gel. It is interesting to point out that whereas the selectivity to epoxide is lower in the case of samples prepared *via* grafting, the selectivity to diol seems not to be influenced by the method of Nb incorporation. However, the selectivity to other products, especially to cyclohexenol, is significantly higher. This phenomena could be explained by a higher impact of radical way in the oxidation carried out on grafted samples, as it was postulated above (the hydrogen peroxide decomposition).

4. Conclusions

In this work the new niobium-containing mesoporous catalysts based on MCF structure were prepared by niobium introduction *via* grafting and co-precipitation. The nature of niobium precursor used for grafting determines the acidity of the catalysts and isolation of Nb. The most bulky ligand (ammonium oxalate) in the Nb source gives rise to the best isolation of niobium species (UV–vis results) and the highest number of acid centres (pyridine adsorption). Niobium-containing MCF materials reveal both acidic and oxidative properties. The first are involved in 2-propanol decomposition and pyridine adsorption, whereas oxidative centres are active in the presence of oxygen and lead to very high selectivity in formaldehyde production from methanol. For liquid phase oxidation of cyclohexene with hydrogen peroxide both kinds of centres are active. Oxidative one causes the formation of epoxide, and acidic sites lead to the ring opening and diol production. The latter is also formed in the solution during homogeneous reaction caused by leaching of Nb species which seems to occur especially from the grafted samples.

Acknowledgements

COST action D36, WG No D36/0006/06, the Polish Ministry of Science (Grant No. 118/COS/2007/03) and KBN grant PBZ-KBN-116/TO9/2004; 2005–2008 are acknowledged for the financial support.

References

[1] P. Schmidt-Winkel, W.W. Lukens Jr., D. Zhao, P. Yang, B.F. Chmelka, G.D. Stucky, J. Am. Chem. Soc. 121 (1999) 254.
[2] P. Schmidt-Winkel, W.W. Lukens Jr., P. Yang, D.I. Marolese, J.S. Lettow, J.Y. Ying, G.D. Stucky, Chem. Mater. 12 (2000) 686.
[3] J. Mrowiec-Bialon, K. Szymanska, K. Maresz, Inż. Chem. Proc. 25 (3–2) (2004) 1367.
[4] N.V. Maksimczuk, M.S. Melgunov, J. Mrowiec-Bialon, A.B. Jarzebski, O.A. Kholdeeva, J. Catal. 235 (2005) 175.
[5] M. Ziolek, Catal. Today 90 (2004) 145.
[6] M. Ziolek, in: P.B. Lawrence (Ed.), Some Aspects of Heterogeneous Catalytic Liquid Phase Oxidation with Hydrogen Peroxide, Nova Science Publishers, Inc., 2006 , p. 73, ISBN: 1-59454-496-4.
[7] J.S. Beck, J.C. Vartuli, W.J. Roth, M.E. Leonowicz, C.T. Kresge, K.D. Schmitt, C.T.-W. Chu, D.H. Olson, E.W. Sheppard, S.B. McCullen, J.B. Higgins, J.L. Schlenker, J. Am. Chem. Soc. 114 (1992) 10834.
[8] W.A. Corvalho, P.B. Varaldo, M. Wallau, U. Schuchardt, Zeolites 18 (1997) 408.
[9] J.M. Fraile, J.I. Garcia, B. Lázaro, J.A. Mayoral, Chem. Commun. (1998) 1807.
[10] M.B. D'Amore, S. Schwarz, Chem. Commun. (1999) 121.
[11] W. Adam, C.M. Mitchell, Ch.R. Saha-Möller, T. Selvam, O. Weichold, J. Mol. Catal. A: Chem. 154 (2000) 251.
[12] L. Nemeth, B. McCulloch, R. Jensen, S. Willson, J. Moscoso, A. Corma, F. Rey, S. Valencia, Stud. Surf. Sci. Catal. 125 (1999) 473.
[13] A. Corma, J.L. Jordá, M.T. Navarro, J. Pérez-Parient, F. Rey, J. Tsuji, Stud. Surf. Sci. Catal. 129 (2000) 169.
[14] A. Corma, M. Domine, J.A. Gaona, J.L. Jorda, M.T. Navarro, F. Rey, J. Perez-Pariente, J. Tsuji, B. McCulloch, L.T. Nemeth, Chem. Commun. (1998) 2211.
[15] I. Nowak, B. Kilos, M. Ziolek, A. Lewandowska, Catal. Today 78 (2003) 487.
[16] B. Kilos, M. Aouine, I. Nowak, M. Ziolek, J.C. Volta, J. Catal. 224 (2004) 314.
[17] J. Xin, J. Suo, X. Zhang, Z. Zhang, New J. Chem. 24 (2000) 569.
[18] B. Kilos, I. Nowak, M. Ziolek, A. Tuel, J.C. Volta, Stud. Surf. Sci. Catal. 158 (2005) 1461.
[19] J. Mrowiec-Białoń, Thermochim. Acta 443 (2006) 49.
[20] R. Brayner, G. Viau, G.M. da Cruz, F. Fiévet-Vincent, F. Fiévet, F. Bozon-Verduraz, Catal. Today 57 (2000) 187.
[21] S. Khabtou, T. Chevreau, J.C. Lavalley, Micropor. Mater. 3 (1994) 133.
[22] E.P. Parry, J. Catal. 2 (1963) 371.
[23] A. Gervasisni, J. Fenyvesi, A. Auroux, Catal. Lett. 43 (1997) 219.
[24] R. Issaadi, F. Garin, Ch.-E. Chitour, Catal. Today 113 (2006) 166.
[25] J.M. Tatibouet, Appl. Catal. A: Gen. 148 (1997) 213.
[26] X. Gao, I.E. Wachs, M.S. Wong, J.Y. Ying, J. Catal. 203 (2001) 18.
[27] M. Trejda, J. Kujawa, M. Ziółek, Catal. Lett. 108 (2006) 141.